

Acceptor spectra of $\text{Al}_x\text{Ga}_{1-x}\text{As}$ -GaAs quantum wells in external fields: Electric, magnetic, and uniaxial stress

W. T. Masselink, Yia-Chung Chang, and H. Morkoç

Coordinated Science Laboratory, University of Illinois at Urbana-Champaign, Urbana, Illinois 61801

(Received 28 May 1985)

We have used the variational method to calculate the acceptor binding energies in GaAs- $\text{Al}_x\text{Ga}_{1-x}\text{As}$ quantum wells with and without the application of electric, magnetic, and uniaxial stress fields. The calculation includes the coupling of the top four valence bands of both materials in the multiband effective-mass approximation. To ensure the convergence of the calculation, a large number of basis functions which are made up of the s -like, p -like, or d -like spatial states multiplied by $j = \frac{3}{2}$ spinors are used for the expansion of the acceptor wave function. Because the quantum well and external field potentials reduce the point-group symmetry from T_d to D_{2d} , the bulk Γ_8 acceptor ground state splits into Γ_6 and Γ_7 states. The Γ_6 state is predominantly derived from the heavy-hole subband and the Γ_7 state is predominantly derived from the light-hole subband. The magnetic field further splits the Γ_6 and Γ_7 states. We have calculated the energies of the Γ_6 state and the Γ_7 state for both center doped and edge doped quantum wells as well as the Γ_6 and Γ_7 valence-subband edges for various barrier heights as functions of well width. In recent studies the photoluminescence resulting from the acceptor levels to conduction-band transition in molecular-beam-epitaxy-grown GaAs- $\text{Al}_x\text{Ga}_{1-x}\text{As}$ superlattices have been measured. Our theoretical results are in excellent agreement with these experimental data.

I. INTRODUCTION

Because of the development and improvement of semiconductor growth techniques such as molecular-beam epitaxy (MBE), the study of artificial semiconductor superlattices has rapidly advanced.^{1,2} The growth rate using MBE is slow enough ($0.3\text{--}8 \text{ \AA s}^{-1}$) that both material composition and intentionally incorporated impurities can be controlled on the atomic scale. In addition, MBE-grown GaAs has a low enough background impurity concentration ($\sim 10^{14} \text{ cm}^{-3}$) that for optical studies the intrinsic characteristics may be dominant. With this low background impurity concentration and monoatomic layer abruptness, recent photoluminescence experiments indicate transition widths at 2 K of less than 0.15 meV for the $\text{Al}_x\text{Ga}_{1-x}\text{As}$ -GaAs system.³

In the GaAs- $\text{Al}_x\text{Ga}_{1-x}\text{As}$ superlattice, so far the most widely studied system, the $\text{Al}_x\text{Ga}_{1-x}\text{As}$ band gap increases with increasing x . How the difference in band gap between GaAs and $\text{Al}_x\text{Ga}_{1-x}\text{As}$ is divided between the conduction band and valence band has been the subject of much study; recent evidence indicates that 65% of the band-gap discontinuity is in the conduction band, with 35% in the valence band.^{4,5} Thus both electrons and holes are confined to rectangularly shaped potential wells in GaAs.

Original studies of this system emphasized the intrinsic properties. More recently, emphasis has been on the extrinsic properties of doped superlattices. Extrinsic transitions may involve donor- and acceptor-bound excitons, donors, and acceptors which could be located at any position in the well or barrier. Although in principle these are no more complicated than in bulk GaAs, material quality

for narrow wells is not as good as for bulk GaAs.

Donor binding energies in quantum wells have been calculated in several approximations. Bastard's original calculation assumed a hydrogenic impurity and infinite barrier height.⁶ Others have made realistic calculations including finite barrier heights.^{7,8} Although Bastard's calculation indicates a continuously increasing binding energy as well width is decreased, these more realistic calculations show that the binding energy goes through a maximum at some nonzero well width. Chaudhuri has recently included the coupling of adjacent quantum wells in a calculation of the donor binding energies.⁹

Very recently, the effect of external perturbations on donors in quantum wells has been studied. In particular, the binding energies of the ground state and several excited states of donors in a magnetic field have been calculated¹⁰⁻¹² as well as the ground-state binding energy of donors in an electric field.¹³ The measured dependence of binding energy with magnetic field seems to agree quite well with these calculations.¹⁴

Calculating the binding energies of acceptors in a superlattice and/or external field is more complicated than for donors because of the more complex valence-band structure. We have previously reported some calculations and measurements of the binding energies of acceptors at the centers and at the edges of GaAs- $\text{Al}_x\text{Ga}_{1-x}\text{As}$ quantum wells.^{15,16} In bulk semiconductor material such as GaAs, the valence band is threefold degenerate at $k=0$, ignoring spin. When spin is included, the degeneracy would be doubled except that the spin-orbit interaction causes two of the bands to be split off. Thus the bulk GaAs valence band is fourfold degenerate at Γ . Away from Γ , the bands split into a twofold-degenerate light-hole band and

a twofold-degenerate heavy-hole band. However, for a quantum well or superlattice, the heavy-hole and light-hole bands are separated even at Γ . In general, however, the coupling between them is still appreciable. In this paper we report a theoretical study of the binding energies of acceptors in $\text{GaAs-Al}_x\text{Ga}_{1-x}\text{As}$ quantum wells which are perturbed by electric, magnetic, or uniaxial stress fields. We include the coupling of the light-hole and heavy-hole bands as well as the finite barriers in the calculation.

II. ACCEPTOR IN A QUANTUM WELL

We begin with the coupled effective-mass equations for the ideal acceptor in bulk material. In this paper an "ideal" acceptor is one in which the total potential due to the impurity center is only the screened Coulomb potential. In the case of infinite spin-orbit coupling, the problem reduces to four coupled equations. For four coupled bands degenerate at $\mathbf{k}=\mathbf{0}$, the most general acceptor Hamiltonian may be written as¹⁷

$$H = \frac{1}{2m_0}(\gamma_1 + \frac{5}{2}\gamma_2)\mathbf{p}^2 - \frac{\gamma_2}{m_0}(p_x^2 J_x^2 + p_y^2 J_y^2 + p_z^2 J_z^2) - \frac{2\gamma_3}{m_0}(\{p_x p_y\}\{J_x J_y\} + \{p_y p_z\}\{J_y J_z\} + \{p_z p_x\}\{J_z J_x\}) - \frac{e^2}{\epsilon_0 r}, \quad (1)$$

where $\{ab\} = (ab + ba)/2$, m_0 is the free-electron mass, \mathbf{p} is the linear momentum operator, \mathbf{J} is the angular momentum operator for the spin- $\frac{3}{2}$ hole, $e^2/\epsilon_0 r$ is the screened Coulomb interaction, and $\gamma_1, \gamma_2, \gamma_3$ are the Luttinger parameters describing the valence band of the material. The kinetic energy term can be written in \mathbf{k} space as

$$\begin{pmatrix} A_- & B & C & 0 \\ B^* & A_+ & 0 & C \\ C^* & 0 & A_+ & -B \\ 0 & C^* & -B^* & A_- \end{pmatrix},$$

where

$$A_{\pm} = \frac{\hbar^2 \gamma_1}{2m_0} \left[\left(1 \pm \frac{\gamma_2}{\gamma_1} \right) (k_x^2 + k_y^2) + \left(1 \mp 2 \frac{\gamma_2}{\gamma_1} \right) k_x^2 \right],$$

$$B = \frac{\hbar^2 \gamma_1}{2m_0} \left[-2\sqrt{3} \frac{\gamma_3}{\gamma_1} (ik_y k_z - k_z k_x) \right], \quad (2)$$

$$C = \frac{\hbar^2 \gamma_1}{2m_0} \left[\sqrt{3} \frac{\gamma_2}{\gamma_1} (k_y^2 - k_x^2) + 2\sqrt{3} \frac{\gamma_3}{\gamma_1} ik_x k_y \right],$$

using the basis described below.¹⁸ In order to adapt this Hamiltonian to the quantum-well problem, we propose an additional term for an acceptor at the center of the well

$$H_1 = \begin{cases} 0 & \text{for } |z| < W/2, \\ V & \text{for } |z| \geq W/2, \end{cases} \quad (3)$$

where V is the valence-band discontinuity between the well material and the barrier material, and W is the well

width. H_1 does not couple different bands because it is spin independent. Although the single-well nature of H_1 makes it more appropriate for completely decoupled quantum wells, this potential will also be appropriate for superlattices with thick barriers because the hole is bound and virtually none of its wave function penetrates through the barriers into the next well. In this calculation, we take $V = 0.35 \Delta E_g(x)$,⁴ where $\Delta E_g(x)$ is the difference in band gaps at $k=0$ between the GaAs and the $\text{Al}_x\text{Ga}_{1-x}\text{As}$ barriers; $\Delta E_g(x)$ is taken to be $1.247x$ eV for $x < 0.45$.¹⁹ In order to find the ground-state energy of the above Hamiltonian using the variational method, a trial wave function that includes the variational parameters must be constructed. Because in this case the location of the acceptor is the center of the well, inversion symmetry is preserved in all three directions. Clearly then, even and odd harmonics will be decoupled. Since we expect the ground state to have even symmetry, only the even harmonics need be included in an expansion of the ground-state hole envelope wave function. This expansion is truncated to include only s - and d -like terms since these are the only terms which will be directly coupled to the s term.

Each term in the effective-mass approximation (EMA) hole wave function is written as a product of a spatial term having either s - or d -like symmetry and a spin- $\frac{3}{2}$ spinor. Thus, there are a total of 24 ($=6 \times 4$) possible types of terms. This number can be greatly reduced by fully exploiting the symmetry through the theory of finite groups.

Bulk GaAs has the symmetry of the tetrahedral point group T_d . The valence-band symmetry may be deduced by coupling the p -like band with the spin- $\frac{1}{2}$ hole. In the T_d symmetry, the p -like band will transform like Γ_5 and the spin- $\frac{1}{2}$ hole like Γ_6 . According to group theory $\Gamma_5 \times \Gamma_6 = \Gamma_7 + \Gamma_8$. The Γ_7 is twofold degenerate and is split off by the spin-orbit coupling. The Γ_8 solution is fourfold degenerate at $\mathbf{k}=\mathbf{0}$, splitting into the heavy-hole and light-hole bands for $\mathbf{k} \neq \mathbf{0}$. The Hamiltonian given above is defined in terms of the four Γ_8 states as given in Ref. 20. Thus

$$\Gamma_8^{3/2} \equiv \begin{pmatrix} 1 \\ 0 \\ 0 \\ 0 \end{pmatrix}, \quad \Gamma_8^{1/2} \equiv \begin{pmatrix} 0 \\ 1 \\ 0 \\ 0 \end{pmatrix}, \quad \Gamma_8^{-1/2} \equiv \begin{pmatrix} 0 \\ 0 \\ 1 \\ 0 \end{pmatrix}, \quad \text{and} \quad \Gamma_8^{-3/2} \equiv \begin{pmatrix} 0 \\ 0 \\ 0 \\ 1 \end{pmatrix}.$$

Using the coupling coefficients of Ref. 20, we couple $\Gamma_5 \times \Gamma_6 = \Gamma_7 + \Gamma_8$ to obtain

$$\begin{aligned} \Gamma_8^{3/2} &= (1/\sqrt{6})(xz + iyz)\uparrow + (i\sqrt{2}/\sqrt{3})xy\downarrow, \\ \Gamma_8^{1/2} &= -(1/\sqrt{2})(xz + iyz)\downarrow, \\ \Gamma_8^{-1/2} &= -(1/\sqrt{2})(xz - iyz)\uparrow, \\ \Gamma_8^{-3/2} &= (1/\sqrt{6})(xz - iyz)\downarrow + (i\sqrt{2}/\sqrt{3})xy\uparrow, \\ \Gamma_7^{1/2} &= (1/\sqrt{3})(xz - iyz)\downarrow - (i/\sqrt{3})xy\uparrow, \\ \Gamma_7^{-1/2} &= -(1/\sqrt{3})(xz + iyz)\uparrow + (i/\sqrt{3})xy\downarrow. \end{aligned} \quad (4)$$

The presence of the quantum well reduces the T_d symmetry to D_{2d} by giving the material one preferred direction. The p -like valence band now transforms like $\Gamma_4 + \Gamma_5$ and the spin- $\frac{1}{2}$ hole transforms like Γ_6 . The product then is $\Gamma_6 + {}^1\Gamma_7 + {}^2\Gamma_7$. Again using the notation of Ref. 20,

$$\begin{aligned}\Gamma_6^{1/2} &= (1/\sqrt{2})(xz + iyz)\downarrow, \\ \Gamma_6^{-1/2} &= (-1/\sqrt{2})(xz - iyz)\uparrow, \\ {}^1\Gamma_7^{1/2} &= -ixz\uparrow, \\ {}^1\Gamma_7^{-1/2} &= ixy\downarrow, \\ {}^2\Gamma_7^{-1/2} &= -(1/\sqrt{2})(xz - iyz)\downarrow, \\ {}^2\Gamma_7^{1/2} &= (1/\sqrt{2})(xz + iyz)\uparrow.\end{aligned}\quad (5)$$

Since the split-off band is Γ_7 -like, we construct from ${}^1\Gamma_7$ and ${}^2\Gamma_7$ new Γ_7 states which are orthogonal to the split-off states, and we find

$$\begin{aligned}\Gamma_8^{3/2} &\rightarrow \Gamma_7^{-1/2}, \\ \Gamma_8^{1/2} &\rightarrow \Gamma_6^{1/2}, \\ \Gamma_8^{-1/2} &\rightarrow \Gamma_6^{-1/2}, \\ \Gamma_8^{-3/2} &\rightarrow \Gamma_7^{1/2},\end{aligned}$$

when the symmetry is reduced from T_d to D_{2d} .

These four spinors must be combined with the one s -like and five d -like spherical harmonics to construct total wave functions which transform like either Γ_6 or Γ_7 . First consider the wave function with overall symmetry of Γ_7 : The first such state is simply a spatial s term with the $\Gamma_7^{1/2}$ or $\Gamma_7^{-1/2}$ spinor. To find the d state, we must consider the product $(\Gamma_6 + \Gamma_7) \times (\Gamma_1 + \Gamma_3 + \Gamma_4 + \Gamma_5)$, since in the D_{2d} group a d state splits into $\Gamma_1 + \Gamma_3 + \Gamma_4 + \Gamma_5$. We find $(\Gamma_6 + \Gamma_7) \times (\Gamma_1 + \Gamma_3 + \Gamma_4 + \Gamma_5) = 5\Gamma_6 + 5\Gamma_7$. Thus there will be five doubly degenerate d -like states and one doubly degenerate s -like state with overall symmetry Γ_7 . As it makes no difference which set of states we choose, we will consider the $\Gamma_7^{-1/2}$ states. The first of these is $\Gamma_7^{-1/2} \times s$,

$${}^0\Gamma_7^{-1/2} = \begin{pmatrix} s \\ 0 \\ 0 \\ 0 \\ 0 \end{pmatrix}.$$

Using the coupling coefficient of Ref. 20, we couple $\Gamma_7 \times \Gamma_1 = \Gamma_7$ and find $\Gamma_7^{-1/2} = \Gamma_7^{-1/2}\Gamma_1$. Since $z^2 - \frac{1}{2}(x^2 + y^2)$ transforms like Γ_1 and is orthogonal to $|s\rangle$,

$${}^1\Gamma_7^{-1/2} = \begin{pmatrix} z^2 - \frac{1}{2}(x^2 + y^2) \\ 0 \\ 0 \\ 0 \end{pmatrix}.$$

Similarly we find ${}^3\Gamma_6^{-1/2} = \Gamma_7^{-1/2}$ and ${}^i\Gamma_4\Gamma_6^{-1/2} = \Gamma_7^{-1/2}$, and so

$${}^2\Gamma_7^{-1/2} = \begin{pmatrix} 0 \\ 0 \\ (\sqrt{3}/2)(x^2 - y^2) \\ 0 \end{pmatrix}, \quad {}^3\Gamma_7^{-1/2} = \begin{pmatrix} 0 \\ 0 \\ ixy \\ 0 \end{pmatrix}.$$

Also

$$(1/\sqrt{2})(\Gamma_5^x\Gamma_6^{1/2} + i\Gamma_5^y\Gamma_6^{1/2}) = \Gamma_7^{-1/2}$$

and

$$-(1/\sqrt{2})(\Gamma_5^x\Gamma_7^{1/2} - i\Gamma_5^y\Gamma_7^{1/2}) = \Gamma_7^{-1/2},$$

so

$${}^4\Gamma_7^{-1/2} = \begin{pmatrix} 0 \\ (1/\sqrt{2})(xz + iyz) \\ 0 \\ 0 \end{pmatrix}$$

and

$${}^5\Gamma_7^{-1/2} = \begin{pmatrix} 0 \\ 0 \\ 0 \\ -(1/\sqrt{2})(xz - iyz) \end{pmatrix}.$$

Referring back to the Hamiltonian, we see that ${}^5\Gamma_7^{-1/2}$ does not couple to any of the matrix elements, so it does not have to be included in the basis. The $\Gamma_7^{-1/2}$ basis is then

$$\begin{pmatrix} s \\ 0 \\ 0 \\ 0 \\ 0 \end{pmatrix}, \quad \begin{pmatrix} z^2 - \frac{1}{2}(x^2 + y^2) \\ 0 \\ 0 \\ 0 \end{pmatrix}, \quad \begin{pmatrix} 0 \\ 0 \\ (\sqrt{3}/2)(x^2 - y^2) \\ 0 \end{pmatrix}, \quad (6)$$

$$\begin{pmatrix} 0 \\ 0 \\ ixy \\ 0 \end{pmatrix}, \quad \begin{pmatrix} 0 \\ (1/\sqrt{2})(xz + iyz) \\ 0 \\ 0 \end{pmatrix}.$$

The $\Gamma_6^{1/2}$ basis is similarly obtained and is related to the $\Gamma_7^{-1/2}$ basis by exchanging the first and second entries and the third and fourth entries. The total Γ_7 variational wave function is written as

$$\langle r | \psi \rangle = \sum_{n=0}^4 {}^n\Gamma_7^{-1/2} \sum_{i=1}^7 C_n(i) e^{-\alpha_i(x^2 + y^2 + \mu z^2)}, \quad (7)$$

where the 35 $C_n(i)$'s are variational parameters, the seven α_i 's are exponents chosen to cover a large physical range, μ is an anisotropy factor which allows the compression of the wave function in the z direction, and ${}^n\Gamma_7^{-1/2}$ are the five spinor-polynomial products given in (6) above. Since μ is also varied to minimize the energy, the calculation uses 36 variational parameters. This is a vast improvement over the 169 parameters which would have been

necessary if we had not simplified the problem using the group theory above.

When the acceptor is in the center of the quantum well there is no question about where the wave function is to be centered. By symmetry it is obvious that the hole wave function would also be centered at the center of the well. With the acceptor at the edge of the quantum well, the hole wave function should be centered between the edge and center of the quantum well because the Coulomb potential tends to pull the hole to the edge of the well while the barrier potentials push it toward the center.

The only change in the Hamiltonian is in H_1 . The quantum-well term is now given by

$$H_1 \equiv \begin{cases} 0 & \text{for } 0 < z \leq W, \\ V & \text{for } z \leq 0 \text{ or } z > W. \end{cases} \quad (8)$$

For the case of the acceptor located at a general position z_0 from the edge of the well,

$$H_1 = \begin{cases} 0 & \text{for } -z_0 < z \leq W - z_0, \\ V & \text{for } z \leq -z_0 \text{ or } z > W - z_0. \end{cases} \quad (9)$$

With the loss of inversion symmetry comes the loss of some of the simplification made when the acceptor is in the center of the well. The ground state will now have p_z terms since only the z direction lacks inversion symmetry. Furthermore, the system symmetry is no longer D_{2d} , so Γ_6 and Γ_7 symmetries are not strictly distinct. By symmetry, $\Gamma_6 p$ states cannot mix with $\Gamma_6 s$ or d states and $\Gamma_7 p$ states cannot mix with $\Gamma_7 s$ or d state. Maintaining the D_{2d} notation, the $\Gamma_6 p_z$ state can, however, mix with the $\Gamma_7 s$ and d states and the $\Gamma_7 p_z$ state can mix with the $\Gamma_6 s$ and d states.

Since this mixing is relatively minor we still denote the state primarily derived from the s and d Γ_7 states as Γ_7 even though it has some Γ_6 character and the state primarily derived from $\Gamma_6 s$ and d state is still denoted Γ_6 . Thus, the additional p_z type of wave-function term is

$$\begin{pmatrix} z \\ 0 \\ 0 \\ 0 \end{pmatrix}$$

for $\Gamma_7^{-1/2}$, and (10)

$$\begin{pmatrix} 0 \\ z \\ 0 \\ 0 \end{pmatrix}$$

for $\Gamma_6^{1/2}$.

The new total Γ_7 variational wave function is written then as

$$\langle r | \psi \rangle = \sum_{n=0}^5 n \Gamma_7^{1/2} \sum_{i=1}^7 C_n(i) e^{-\alpha_i [x^2 + y^2 + \mu(z-q)^2]}, \quad (11)$$

where

$${}^5\Gamma_7^{-1/2} = \begin{pmatrix} z \\ 0 \\ 0 \\ 0 \end{pmatrix}$$

and q is a new variational parameter which allows the wave function to be centered at an arbitrary position. For the case of the center doped acceptor, $z_0 = W/2$, $q = 0$, and $C_5(i) = 0$. This shifted ellipsoidal Gaussian set has the ability of reproducing reasonably well the bound-hole wave function when the Coulomb center is at any point in the well for any well thickness.

The ground-state energy and wave function is obtained by numerically solving Schrödinger's equation $H\psi = E_S\psi$, where S is the overlap matrix. This means solving a 35×35 secular equation if ψ has been expanded as in Eq. (7) for a center-doped well or a 42×42 secular equation if ψ has been expanded as in Eq. (11) for an arbitrarily placed acceptor. The values of μ and, in Eq. (11), q , are varied until the energy E is minimized. The resulting lowest energy eigenvalue is the Γ_6 or Γ_7 variational acceptor ground-state energy as measured from the bulk valence-band edge.

In order to account for the difference in effective-mass parameters and dielectric constants in the two materials, GaAs and $\text{Al}_x\text{Ga}_{1-x}\text{As}$, the problem is solved twice for each well width and barrier composition. We define

$$f_1 = \int_{-\infty}^{\infty} dx \int_{-\infty}^{\infty} dy \int_{-z_0}^{W-z_0} |\psi|^2 dz$$

as the fraction of hole-envelope wave function in the quantum well assuming the GaAs parameters, and similarly f_2 as the fraction of hole-envelope wave function in the quantum well assuming the $\text{Al}_x\text{Ga}_{1-x}\text{As}$ parameters. The actual fraction of hole wave function in the well, f , requires $f = ff_1 + (1-f)f_2$. Thus $f = f_2 / (1 + f_2 - f_1)$. The actual acceptor energy then is $E = fE_1 + (1-f)E_2$, where E_1 is the acceptor energy assuming the GaAs parameters and E_2 is the acceptor energy assuming the $\text{Al}_x\text{Ga}_{1-x}\text{As}$ parameters. Although this is not an ideal method for treating the boundary condition, the exact details of how the total wave function is matched across the interface will have very little effect on the energies. This is due to the fact that in a variational calculation, first-order changes in wave function result in only second-order changes in energy.

In order to calculate the binding energy for the acceptor, we also calculate the Γ_6 and Γ_7 (heavy hole and light hole) subband edges as measured from the bulk valence-band edge using the same Hamiltonian with the impurity potential excluded. The Γ_7 acceptor binding energy is then the difference between the Γ_7 subband edge and the Γ_7 acceptor energy, both measured from the same reference energy. The method for finding the Γ_6 binding energy is identical to that for the Γ_7 binding energy described above except that the Γ_6 -symmetry wave function is used.

We study GaAs- $\text{Al}_x\text{Ga}_{1-x}\text{As}$ center and edge acceptor-doped quantum wells with two different barrier alloy compositions: $x = 0.10$ and 0.30 . The Luttinger parameters and dielectric constants are taken to be

$$\epsilon_0=12.35, \gamma_1=7.65, \gamma_2=2.41, \gamma_3=3.28$$

for GaAs and

$$\epsilon_0=9.80, \gamma_1=4.04, \gamma_2=0.78, \gamma_3=1.57$$

for AlAs.²¹ For the alloys, we use a linear interpolation between those of GaAs and of AlAs for all four parameters.

The heavy- and light-hole subband energies along with the Γ_6 and Γ_7 acceptor energies are shown as functions of well width in Fig. 1. This calculation assumes the Al mole fraction x to be 0.30 and is for an acceptor in the center of the well. The difference between the Γ_6 (heavy-hole) subband energy and the Γ_6 acceptor energy is the Γ_6 acceptor binding energy. The Γ_7 (light-hole) acceptor binding energy is similarly defined. One can also discern from this figure the energy difference between the Γ_7 and Γ_6 acceptor states; this energy difference can be measured using Raman spectroscopy. The calculated acceptor binding energies are shown for the two alloy compositions (0.1 and 0.3) and both symmetries (Γ_6 and Γ_7) as functions of the well width in Fig. 2. In all cases the binding energy reaches a maximum at a nonzero well width which is similar to that calculated for donors^{7,8} and excitons²² in finite-barrier-height quantum wells. As expected, a higher barrier Al mole fraction results in a greater binding energy. In the bulk limit, the binding energy for all six cases is 27.1 meV, which is consistent with previously calculated and measured acceptor binding energies in bulk GaAs. As the quantum-well effects become important, the binding energy of the Γ_7 ground state is greater than that of the Γ_6 ground state. We see that the barrier height is less important in determining the binding energy than is the symmetry. For narrower wells, the effect of the hole confinement is more pronounced, leading to increasing binding energies. The maximum binding energy occurs at well widths between 5 and 50 Å, depending on the barrier height and symmetry. The maximum binding energy

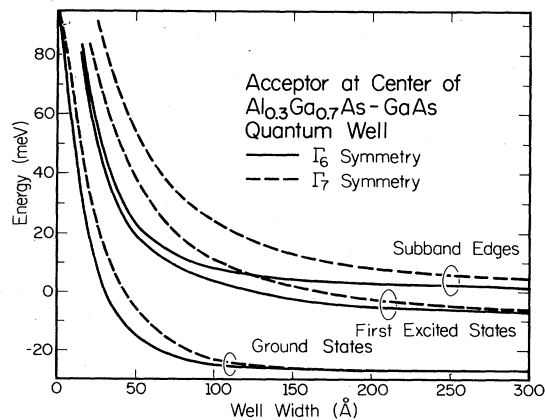


FIG. 1. Energies of the valence-band edges, ground-state acceptor energies, and first excited-state acceptor energies as functions of well width for acceptors in the center of GaAs-Al_{0.3}Ga_{0.7}As quantum wells. Positive energy is measured up from zero and the valence-band discontinuity is assumed to be 35% of the band-gap discontinuity between GaAs and AlGaAs.

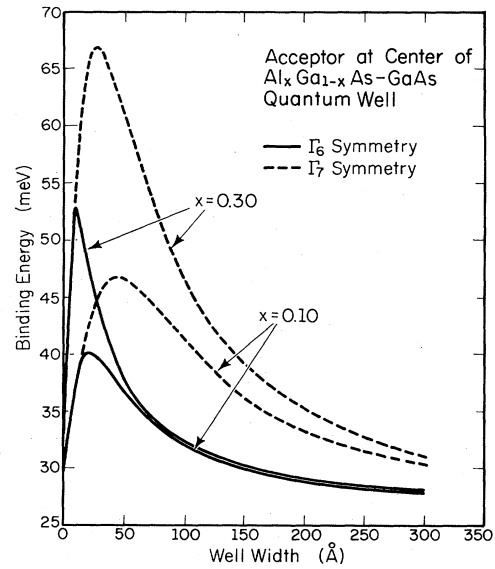


FIG. 2. Binding energies of the center doped ideal acceptor ground states as functions of well width for two barrier heights and both symmetries. The Γ_6 binding energy is measured from the top of the heavy-hole subband and the Γ_7 binding energy is measured from the top of the light-hole subband.

occurs at larger well width for smaller mole fractions and for the Γ_7 symmetry. When the well width is zero, then all that is left is bulk Al_xGa_{1-x}As and the binding energy is, of course, simply that of the alloy. In this limit, the Γ_6 and Γ_7 solutions are again degenerate.

Figure 3 shows the squares of the heavy-hole envelope wave function for different well widths in GaAs-Al_{0.3}Ga_{0.7}As quantum wells when the Coulomb center is

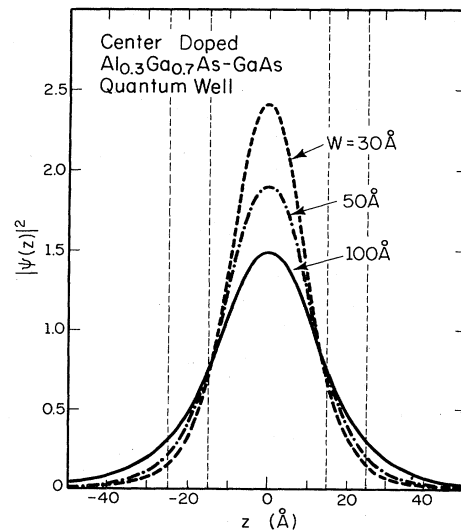


FIG. 3. On-center acceptor ground-state envelope wave function squared, plotted along the axis normal to the interfaces for different GaAs well thicknesses. The Coulomb potential is located at $z=0$ and the vertical dashed lines indicate the heterointerfaces.

located at $z=0$ and the wave function has been integrated over x and y . As one expects, narrower wells cause the hole to be more confined and peaked at the center of the well. For well widths greater than about 200 Å, the $\text{Al}_x\text{Ga}_{1-x}\text{As}$ barriers no longer substantially affect the acceptor wave function. The reason the acceptor binding energy continues to depend on well width for widths greater than 200 Å is that the quantized subband edges depend on well width (see Fig. 1). When the hole is bound to the acceptor, the Coulomb force alone confines the hole quite well to within 100 Å of the acceptor center and, therefore, wide wells do not affect the wave function. Without the Coulomb potential, however, only the $\text{Al}_x\text{Ga}_{1-x}\text{As}$ barriers serve to confine the hole and naturally the unbound hole energy continues to depend on well width.

We have also investigated acceptors located at the edge of a quantum well. Figure 4 shows the valence-band edges and edge doped acceptor energies for both symmetries again assuming $x=0.30$. Although not separately plotted, the energy difference between the Γ_6 and Γ_7 acceptor ground states can also be discerned from Fig. 4. Preliminary results from Raman spectroscopy indicate that this transition is observable and is in relatively good agreement with the calculation.²³

The difference between subband energy and acceptor energy, the acceptor binding energy, is displayed in Fig. 5 for the two mole fractions and both symmetries. Again, the Γ_6 symmetry is that of the heavy hole and the Γ_7 symmetry is that of the light hole although in this case there is a small amount of mixing (about 1%). We find that the edge-doped acceptor's binding energies are smaller than the center-doped acceptors, just as Bastard found.

Figure 6 shows the squares of the heavy-hole-envelope wave function for different well width in $\text{GaAs-Al}_{0.3}\text{Ga}_{0.7}\text{As}$ quantum wells when the Coulomb center is located at the edge of the quantum wells and the wave

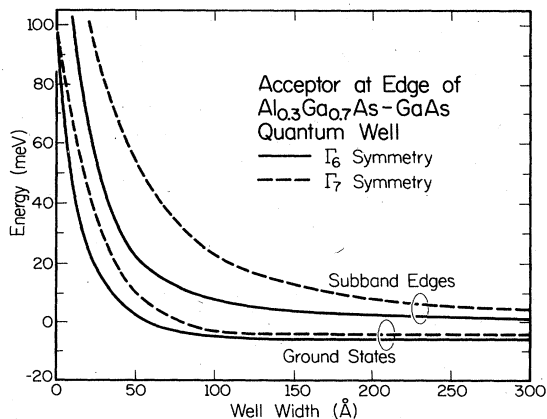


FIG. 4. Energies of the valence-band edges and of the ground-state acceptors located at the edges of $\text{GaAs-Al}_{0.3}\text{Ga}_{0.7}\text{As}$ quantum wells plotted as functions of well width. Positive energy is measured from zero (which corresponds to the bulk valence-band edge) and the valence-band discontinuity is taken to be 35% of the total band-gap discontinuity between GaAs and AlGaAs.

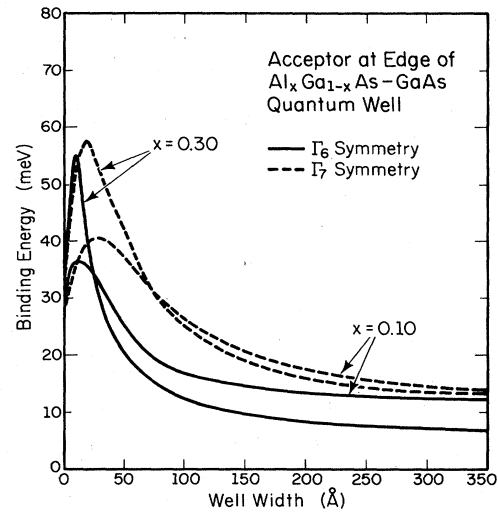


FIG. 5. Binding energies of the edge doped ideal acceptor ground states as functions of well width for two barrier heights and both symmetries. The Γ_6 binding energy is measured from the top of the heavy-hole subband, and the Γ_7 binding energy is measured from the top of the light hole subband.

functions are integrated over x and y . Again, narrower wells cause the hole to be more spatially confined and peaked closer to the center of the well.

Using the quantum-well term in the Hamiltonian given in (9), we are able to study the dependence of the acceptor binding energy on z_0 . The two limiting cases—center and edge—have already been described. In all cases, the maximum binding energy occurs when the acceptor is at the center of the well, and the minimum binding energy occurs when the acceptor is at the edge of the well. Figure 7 shows the position dependence of the binding energy

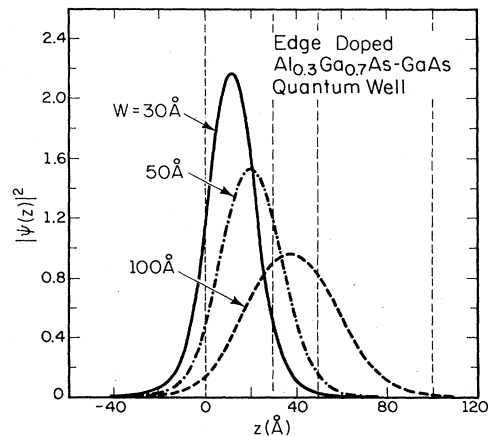


FIG. 6. On-edge acceptor ground-state envelope wave function squared plotted along the axis normal to the interfaces for different GaAs well thicknesses. The Coulomb potential is located at $z=0$ and the vertical dashed lines indicate the heterointerfaces.

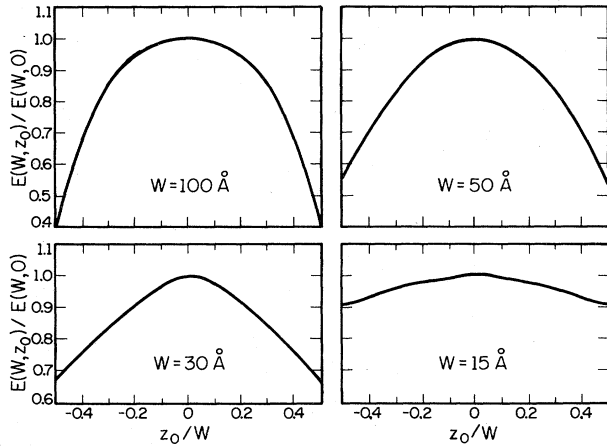


FIG. 7. Position dependence of the heavy-hole acceptor binding energy in an $\text{Al}_{0.3}\text{Ga}_{0.7}\text{As}$ -GaAs quantum well for several well thicknesses.

of acceptors in $\text{Al}_{0.3}\text{Ga}_{0.7}\text{As}$ -GaAs quantum wells of width 100, 50, 30, and 15 Å. For wider wells the binding energy is much more position dependent than for narrower wells. These results are in qualitative agreement with those of Fig. 2 of Ref. 6. The very small value of dE/dz_0 near the center of the well implies that a relatively large number of acceptor centers near the center of the well will all have about the same binding energies. This explains why the center acceptor binding energy is relatively easy to experimentally measure. Near the edge of the well, on the other hand, dE/dz_0 is large, and therefore at a given energy there are far fewer acceptors. Bastard has in the hydrogenic model calculated a density of impurity state per unit binding energy,

$$g_L(E) = \frac{2}{L} \left| \frac{dz_0}{dE} \right|. \quad (12)$$

Again our results are qualitatively identical to his. Since dE/dz_0 vanishes at the center of the well, g_L becomes infinite at the center. At the edge of the well, g_L is larger for smaller well widths and for $W=15$ Å is even peaked at the edge. This explains why the edge binding energy is more easily seen in uniformly doped samples when the wells are narrow.

Several experimental studies have been made of the acceptor binding energies in $\text{Al}_x\text{Ga}_{1-x}\text{As}$ -GaAs quantum wells. The samples in Refs. 24 and 25 were uniformly doped throughout the wells with either carbon or beryllium. The carbon-doped samples were unintentionally doped, utilizing the unavoidable carbon background in MBE-grown GaAs. In the studies conducted by the authors in Refs. 15 and 16, the wells were selectively doped with beryllium at either the centers or edges of the wells.

Since the different acceptors have different bulk binding energies, an additional term is added to the Hamiltonian to provide a short-ranged potential. This potential takes the form of $H_c = Ue^{(-r/r_0)^2}$, where $r_0 = 1$ Å and U is chosen so the bulk GaAs acceptor binding energy is shifted from 27.1 meV with $U=0$ to either 26.0 meV for

carbon or 28.0 meV for beryllium. The choice of r_0 is not at all critical; a different r_0 would, however, necessitate using different values of U as well.

For the Γ_6 -center acceptor calculation with $x=0.3$, H_c was included with $U=8.00$ eV for carbon and $U=-5.55$ eV for beryllium. Figure 8 shows the calculated binding energies for center doped carbon and beryllium in GaAs- $\text{Al}_{0.3}\text{Ga}_{0.7}\text{As}$ quantum wells and the binding energy of an ideal ($U=0$) edge doped acceptor. Included also is experimental data measured by us and from Refs. 24 and 25. The four points near the edge doped curve are believed to be due to edge doped acceptors; those measured by us were intentionally doped only at the edge of the wells. Clearly, these experimental data measured by us and by others are in very good agreement with the calculations.

In particular, the measured energy of about 50 meV for Be acceptors in the centers of 30-Å quantum wells is quite consistent with the present calculation. A similar calculation reported earlier by us^{15,16} using a smaller valence-band discontinuity [$\Delta E_v = 0.15\Delta E_g(x)$] showed a serious discrepancy at this point. Comparing these calculations, we see that using the present valence-band discontinuity of 35% instead of the previously accepted one of 15% does not affect the binding energy in wells wider than about 100 Å. At 30 Å, however, there is a significant difference between these calculations, with the present one in much better agreement. Because of the sensitivity of the acceptor energy to valence-band offset, this data provides further evidence that the valence-band discontinuity is much greater than 15% of the total band-gap discontinuity and is around 35% as others have recently measured.^{4,5} Raman spectroscopy experiments measuring

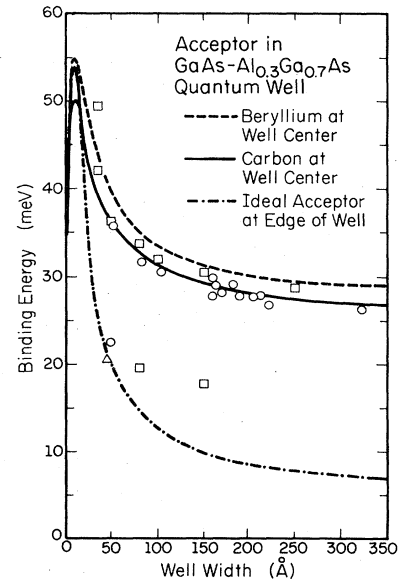


FIG. 8. Calculated energy of the heavy-hole center doped beryllium and carbon acceptors, the heavy-hole edge doped ideal acceptor in $\text{Al}_{0.3}\text{Ga}_{0.7}\text{As}$ -GaAs quantum wells, and experimental data. The data indicated by squares are for selectively doped beryllium measured by the authors, the circles are for carbon from Ref. 24, and the triangle is for beryllium from Ref. 25.

both the Γ_6 ground state to the Γ_6 band edge and also the Γ_6 ground state to the Γ_6 first excited state also appear to agree with these photoluminescence measurements and calculations.²³

III. ACCEPTOR IN A QUANTUM WELL WITH AN ELECTRIC FIELD

In this section we consider the effect of an externally applied electric field on the acceptor in a quantum well. By restricting ourselves to fields applied in the z direction, the symmetry remains that of the off-center acceptor in a quantum well with no field. As a consequence of the electric field, an additional term must be added to the Hamiltonian given in Eqs. (1) and (9). The term due to the electric field may be written

$$H_2 = \mathcal{E}z, \quad (13)$$

where \mathcal{E} is the field strength.

In the related hydrogenic system, such a term results in the well-known Stark effect. In the Stark effect, no state is truly a bound state since the potential becomes arbitrarily negative for values of z far from the origin. Despite this, there are resonant states which closely resemble the bound hydrogenic states in the absence of an electric field. The binding energy of these states is considered then to be the difference in energy between that state and the continuum with no field. In any first-order approach, such as first-order perturbation theory, the ground-state $1s$ level is not affected by an electric field since the $1s$ state has even parity and the electric field has odd parity. The ground state is, however, lowered by the electric field when one allows higher lying odd-parity states to couple to the $1s$ state through the field. For small fields, this coupling results in an energy shift proportional to \mathcal{E}^2 . For large fields an \mathcal{E}^1 term becomes dominant. The donor spectrum, when considered within the effective-mass approximation (EMA), is extremely similar to the hydrogenic spectrum. The theory of the Stark shift is similarly related with the quasibound states being measured from the low-energy edge of the conduction band.

A major difference between the donor and acceptor Stark effects is that the unperturbed donor ground state is quite well described by a single spherical symmetry; the acceptor ground state already includes coupling between s and d states. The additional coupling of p states through the electric field will, thus, be largely masked for small fields.

Rather than relying on perturbation theory, we solve for the ground-state acceptor energy in an electric field using the variational method. This is done by restricting the basis to orbitals centered near the Coulomb potential and sufficiently located so that the lowest state calculated resembles the unperturbed ground state. Figure 9 shows the effect of an electric field on the bulk ground-state acceptor binding energy. The binding energy is measured from the valence-band edge where the electric potential is zero. Also reported in Fig. 9 is the energy assuming a hy-

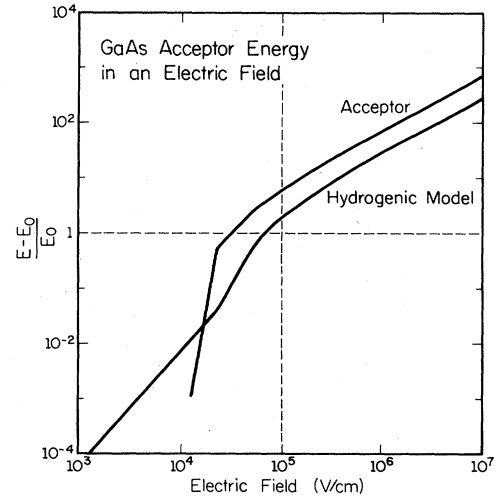


FIG. 9. The relative change in acceptor energy as a function of electric field. The curve labeled "acceptor" is for an actual GaAs acceptor; the curve labeled "hydrogenic" is for a hydrogenic system with the same dielectric constant and binding energy as the GaAs acceptor.

drogenic system with the same binding energy and dielectric constant as the GaAs acceptor we have studied. At small electric fields, the acceptor is virtually unaffected by the field and the hydrogenic energy shift is proportional to \mathcal{E}^2 . At large fields, both the acceptor and hydrogenic-system energies depend on \mathcal{E} as \mathcal{E}^1 . At midfields the acceptor energy changes rapidly with field, making the transition from being virtually unaffected by the field to its high-field value.

The effect of the electric field on the acceptor in a quantum well is qualitatively like the effect on the bulk

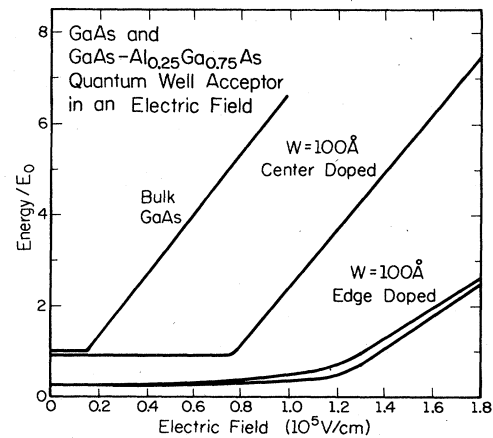


FIG. 10. The absolute values of the acceptor energy measured from the bulk valence band as functions of electric field for an acceptor in GaAs and acceptor in an $\text{Al}_{0.25}\text{Ga}_{0.75}\text{As}$ -GaAs quantum well. The edge doped acceptor is split because the two edges are not degenerate in an electric field.

acceptor. As shown in Fig. 10, the quantum-well case requires a much larger field in order to observe any energy shift. Once the critical field needed to shift the acceptor energy is reached, however, the derivative of acceptor energy with respect to field is approximately the same as in the bulk case. The reason for the larger field required for the onset of the energy shift is that the quantum-well potential further lifts the energies of the p -like orbitals whose coupling is responsible for the energy shift.

$$\frac{\hbar^2}{2m_0} \left\{ (\gamma_1 + \frac{5}{2}\gamma_2)k^2 - 2\gamma_2(k_x^2 J_x^2 + k_y^2 J_y^2 + k_z^2 J_z^2) - 4\gamma_3(\{k_x k_y\}\{J_x J_y\} + \{k_y k_z\}\{J_y J_z\} + \{k_z k_x\}\{J_z J_x\}) - \frac{2e}{\hbar c} \kappa \mathbf{J} \cdot \mathbf{B} \right\} - e^2/\epsilon r. \quad (14)$$

In this expression, $\mathbf{K} = i\nabla + e/2c(\mathbf{B} \times \mathbf{r})$, $\kappa = 1.72$, $\mathbf{B} = B\mathbf{z}$, and the other expressions are the same as in (1).²⁷

In the hydrogenic system, a magnetic field results in the Zeeman effect.²⁸ This problem is simpler because L_z and S_z are maintained as good quantum numbers. Because of this, the Zeeman-effect Hamiltonian can be simplified to

$$\frac{\hbar}{2m} k^2 + \frac{eB}{2mc} (L_z + 2S_z) + \frac{e^2 B^2}{8mc^2} (x^2 + y^2), \quad (15)$$

where B is in the z direction. Since S_z is generally conserved, the term involving S_z also appears in the free-particle Hamiltonian and may be neglected in the calculation of the binding energy.

In the acceptor system, neither L_z nor S_z are well defined. Figure 11(a) shows the ground state and first excited Γ_6 states (D_{2d} symmetry) for an acceptor in a magnetic field. For zero field, the Γ_6 states correspond to Γ_8 states in the T_d symmetry. The calculation is for two cases: $\kappa=0$ and $\kappa=1.72$, the actual value. Looking at the $\kappa=0$ line, one can deduce an effective L_z by looking at the slope of this curve in the small-field limit. Our calculation indicates the effective L_z to be 0.76 and 0.69 for the ground and excited states, respectively. This is reasonable since the wave function is largely composed of s -like orbitals, but with d -like orbitals as well. The difference between the $\kappa=0$ and $\kappa=1.72$ curves can be similarly used to deduce an effective J_z . The difference between the acceptor energies with $\kappa=0$ and $\kappa=1.72$ is given by

$$\frac{\hbar e}{cm_0} \kappa J_z^{\text{eff}} B$$

from Eq. (14). In this expression J_z^{eff} is the effective J_z , $\kappa=1.72$, and B is the field. We find the effective J_z to be 1.15 and 1.12 for the ground and excited states. This again is reasonable since the wave function is composed of $J = \frac{3}{2}$ and $\frac{1}{2}$ spinors and is primarily derived from the $J_z = +\frac{3}{2}$ state. Similarly Fig. 11(b) shows the acceptor energies for $\kappa=0$ and 1.72 in the Γ_7 symmetry. As in the previous case, at $B=0$ the solution corresponds to the Γ_8 -symmetry solution on the T_d symmetry. The effective L_z deduced in this case is 0.32 and 0.28 for the ground and excited states. This again indicates a wave function composed primarily of $L_z=0$ orbitals. The effective J_z is about 0.4 for both ground and excited states. This is also reasonable since these states are primarily composed of $J_z = +\frac{1}{2}$ spinors with some contribution from the $J_z = -\frac{3}{2}$ spinors.

IV. ACCEPTOR IN A QUANTUM WELL WITH A MAGNETIC FIELD

In this section, we calculate the effect of a magnetic field on the acceptor ground state in a quantum well. As in the case of the electric field, we restrict ourselves to fields applied along the z direction. The symmetry in this case is D_{2d} and the basis is identical to that given in Eq. (6). The Hamiltonian for the bulk acceptor given similarly to Eq. (1) by²⁶

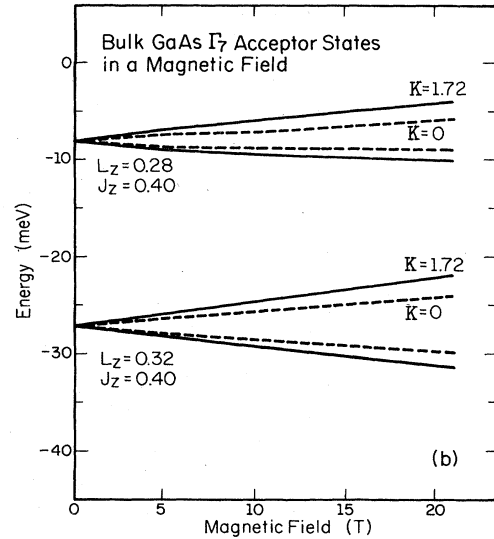
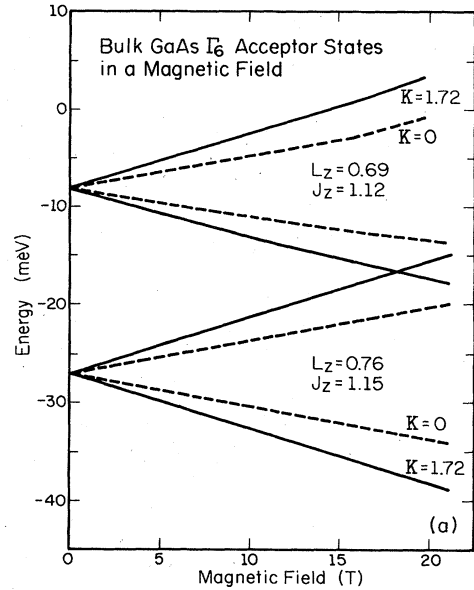


FIG. 11. The GaAs acceptor energies with (a) Γ_6 and (b) Γ_7 symmetries as functions of magnetic field. At zero field, all solutions correspond to the Γ_8 representation in the T_d space group. The energies are calculated both with $\kappa=0$ and $\kappa=1.72$ [see Eq. (14)] so that an effective L_z and J_z can be determined.

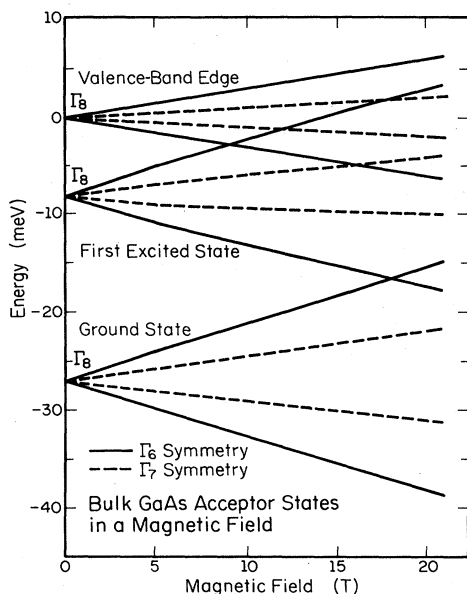


FIG. 12. The GaAs acceptor energies and valence-band edges as functions of magnetic field. Shown are all four symmetries, $\Gamma_6^{1/2}$, $\Gamma_6^{-1/2}$, $\Gamma_7^{1/2}$, $\Gamma_7^{-1/2}$. The binding energy for a given symmetry is the difference between the acceptor state and band edge for that symmetry.

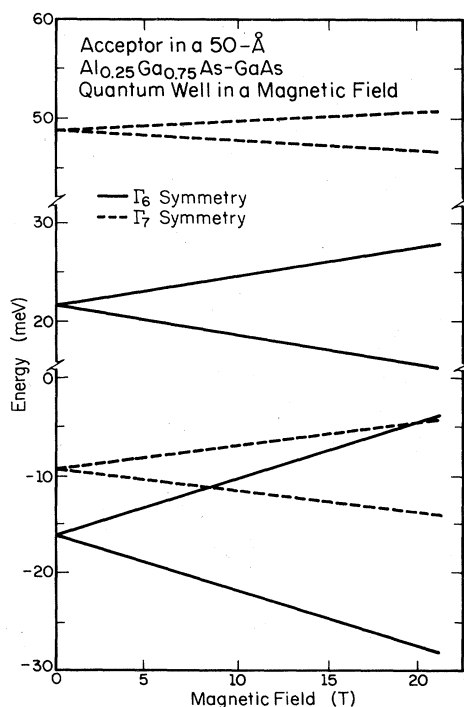


FIG. 13. The Γ_6 and Γ_7 acceptor energies and valence-band edges for the GaAs- $\text{Al}_{0.25}\text{Ga}_{0.75}\text{As}$ quantum-well system in a magnetic field. Because of the quantum well, the fourfold degeneracy is lifted already at $B=0$; the derivative of energy with respect to field is virtually identical to that of the acceptor in bulk GaAs.

Figure 12 shows the acceptor energies and the valence-band edges for both symmetries as functions of magnetic field. The binding energy for a given symmetry is the difference between the acceptor energy and band edge for that symmetry. For each nonzero magnetic field, the four energies for each state correspond to the $\Gamma_6^{\pm 1/2}$, $\Gamma_6^{-1/2}$, $\Gamma_7^{\pm 1/2}$, and $\Gamma_7^{-1/2}$ symmetries which converge to the fourfold-degenerate Γ_8 symmetry state at zero field.

In a quantum well, already at zero field the Γ_8 state is split into the two twofold-degenerate states Γ_6 and Γ_7 as we saw in Sec. II. The presence of a magnetic field splits these states and further shifts their energies. Figure 13 shows the ground-state acceptor energies for an acceptor at the center of a 50-Å well in a magnetic field. Although the Γ_6 and Γ_7 symmetries are distinct already at $B=0$, the splitting due to the field is practically identical to that of the bulk acceptor for each symmetry. In fact, even in narrow wells the effective L_z and J_z remain practically identical to those described earlier for the bulk acceptor. This general result should be valuable for the analysis of magnetic field measurements on GaAs acceptors both in bulk GaAs and in quantum wells.

V. ACCEPTOR IN A QUANTUM WELL WITH UNIAXIAL STRESS

In this section, we consider the effect of compressive uniaxial stress along the growth (z) direction on the acceptor spectrum in quantum wells. The stress contributes to an additional term, H_s , to the Hamiltonian described in (1). In terms the strain tensor ϵ_{ij} , H_s can be written as²⁹

$$H_s = D_d(\epsilon_{xx} + \epsilon_{yy} + \epsilon_{zz}) + \frac{2}{3}D_u[(J_x^2 - \frac{1}{3}J^2)\epsilon_{xx} + \text{c.p.}] + \frac{4}{3}D'_u(\{J_x J_y\}\epsilon_{xy} + \text{c.p.})$$

where D_d , D_u , and D'_u are deformation potentials which can be determined experimentally for bulk GaAs. Here the symbol c.p. stands for cyclic permutation of x, y, z . We assume these deformation potentials for GaAs- $\text{Al}_x\text{Ga}_{1-x}\text{As}$ quantum wells are the same as those for bulk GaAs.

For a uniaxial stress with strength X applied in the z direction, the strain tensor is given by $\epsilon_{xy} = \epsilon_{yz} = \epsilon_{zx} = 0$, $\epsilon_{xx} = \epsilon_{yy} = S_{12}X$, and $\epsilon_{zz} = S_{11}X$, where S_{11} and S_{12} are two components of the compliance tensor. Substituting these expressions in and expressing H_s in the spin- $(-\frac{3}{2})$ basis states, we have

$$\langle \pm \frac{3}{2} | H_s | \pm \frac{3}{2} \rangle = d + \delta$$

and

$$\langle \pm \frac{1}{2} | H_s | \pm \frac{1}{2} \rangle = d - \delta,$$

where

$$d = D_d(S_{11} + S_{12})X$$

and

$$\delta = D_u(S_{11} - S_{12})X/3.$$

Using the values $S_{11} = 1.159$, $S_{12} = -0.368$ (in 10^{-12} cm^2/dyn), and $D_u = 3.66$ eV for bulk GaAs,^{30,31} we have $\delta = 1.86X$ meV, if X is measured in units of kbar.

The calculation of the acceptor spectrum in GaAs-

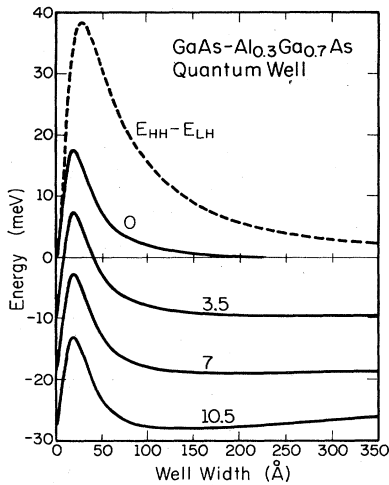


FIG. 14. Energy separation between the Γ_6 acceptor state and the Γ_7 acceptor state [$E_A(\Gamma_6) - E_A(\Gamma_7)$] versus well width for a number of applied uniaxial stresses, $x = 0, 3.5, 7,$ and 10.5 kbar. The energy separation between the zone center heavy-hole (HH) and light-hole (LH) subband states ($E_{HH} - E_{LH}$) is also shown in the dashed curve.

$Al_xGa_{1-x}As$ quantum wells follows the same prescription as described in Sec. II. The results for center doped ideal acceptors are presented in Figs. 14 and 15. Figure 14 shows the energy separation between the lowest energy level of Γ_6 and Γ_7 symmetries as a function of the GaAs well width, for uniaxial stresses from 0 to 10.5 kbar (solid curves). Also included for comparison is the separation between the first heavy-hole and light-hole subband energies at the zone center (dashed).

Figure 15 shows the binding energies of the acceptor states with Γ_6 symmetry and Γ_7 symmetry for uniaxial stresses from 0 to 10.5 kbar. The Γ_6 and Γ_7 acceptor-state binding energies are defined with respect to the first heavy-hole (HH) and light-hole (LH) subband energies at zone center, respectively. For comparison, the differences for the subband energies $E_{HH} - E_{LH}$ and $E_{LH} - E_{HH}$ are also shown as dashed curves in 15(a) and 15(b), respectively. Note that the differences between the solid curves and the dashed curves would give rise to the binding energies with respect to the lowest subband energies at the zone center. We find that the Γ_6 acceptor binding energy increases while the Γ_7 acceptor binding energy decreases with increasing uniaxial stress. This is because the light-hole subband energy approaches the heavy-hole subband energy as the stress increases and since Γ_6 (HH) acceptor state contains a fraction of light-hole (LH) character, its energy is pushed further away from the HH subband, whereas since Γ_7 (LH) acceptor state contains a fraction of heavy-hole (HH) character, its energy is pulled closer toward the LH subband. As can be seen from Fig. 15, the dependence of binding energy on the stress is not linear.

VI. CONCLUSIONS

We have calculated the acceptor spectra in GaAs- $Al_xGa_{1-x}As$ quantum wells with no external fields and with electric, magnetic, or uniaxial stress field, using the varia-

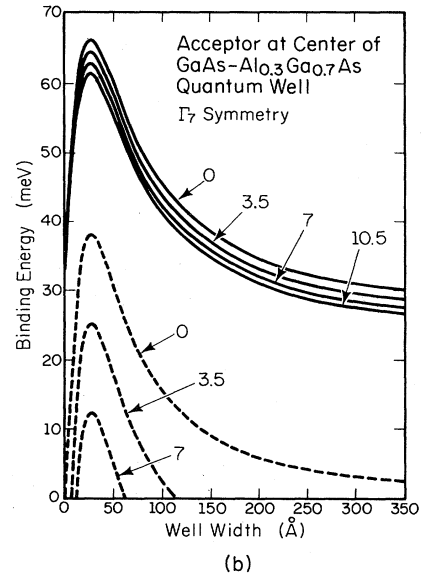
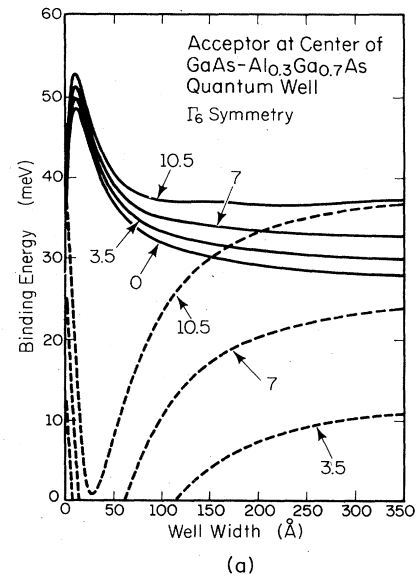


FIG. 15. Binding energies of center doped acceptor states versus well width for $x = 0, 3.5, 7,$ and 10.5 kbar; (a) Γ_6 symmetry (heavy-hole-like), (b) Γ_7 symmetry (light-hole-like). The dashed curves show $E_{HH} - E_{LH}$ in (a) and $E_{LH} - E_{HH}$ in (b).

tional method. This calculation includes the coupling of the top four valence bands of both materials in the multi-band effective-mass approximation. The ground states and some excited states for both heavy- and light-hole acceptors at the centers and edges of quantum wells have been calculated for various Al mole fractions as functions of the well width. Our experimental determination of the binding energies as well as experimental data from other laboratories agree very well with these calculations. By comparing the experimental and theoretical binding energies for narrow wells, we can also determine the approximate valence-band discontinuity. Our calculations using the recent experimental value of $\Delta E_v = 0.35\Delta E_g$ are in

good agreement with the available experimental data, including those obtained from narrow-well systems.

In addition, we report the first calculation of acceptor energies in electric, magnetic, and uniaxial stress fields in quantum wells as well as bulk GaAs. The effect of an electric field on an acceptor is to lower the total acceptor energy; the onset of this effect is rather abrupt. The presence of a quantum-well potential increases the electric field necessary for a similarly abrupt onset of the lowering of the total acceptor energy. The magnetic field splits the bulk GaAs Γ_8 state into its four components; the energies of these states vary fairly linearly at accessible laboratory fields. In a quantum well, the Γ_8 state is already split into two distinct states even at zero magnetic field. Application of the magnetic field further splits these states almost exactly as they were split in the bulk crystal. Application of uniaxial stress increases the binding energy of the heavy-hole acceptor, but reduces the binding energy of the light-hole acceptor. Sufficient stress can even raise the

heavy-hole state above the light-hole state, allowing the possibility of a detailed study of the light-hole acceptor. All of these cases should serve as useful guides for the interpretation of experimental data involving semiconductor acceptor states in external fields.

ACKNOWLEDGMENTS

The authors are grateful to R. Fischer for growing some of the superlattice structures investigated here and to the Materials Research Laboratory for the use of its computing facilities. The authors also acknowledge useful discussions with R. Merlin, D. Gammon, K. Bajaj, and M. Chandrasekar and access to the laboratories of M. Klein. This work was supported by the U. S. Office of Naval Research under Contract No. N00014-81-K-0430 and by the U. S. Air Force Office of Scientific Research under Contract No. F49620-83-K-0021. W. T. Masselink is supported in part by IBM.

¹*Molecular Beam Epitaxy and Heterostructures*, edited by L. L. Chang and K. Ploog (Nijhoff, Dordrecht, 1985).

²For a review, see R. Dingle, in *Festkörperprobleme, Advances in Solid State Physics*, edited by H. J. Queisser (Pergamon-Vieweg, Braunschweig, 1975), Vol. 15, pp. 21–48.

³D. C. Reynolds, K. K. Bajaj, C. W. Litton, P. W. Yu, W. T. Masselink, R. Fischer, and H. Morkoç, *Phys. Rev. B* **29**, 7038 (1984).

⁴D. Arnold, A. Ketterson, T. Henderson, J. Klem, and H. Morkoç, *Appl. Phys. Lett.* **45**, 1237 (1984).

⁵H. Okumura, S. Misawa, S. Yoshida, and S. Gondou, *Appl. Phys. Lett.* **46**, 377 (1985).

⁶G. Bastard, *Phys. Rev. B* **24**, 4714 (1981).

⁷C. Mailhot, Y. C. Chang, and T. C. McGill, *J. Vac. Sci. Technol.* **21**, 519 (1982); *Phys. Rev. B* **26**, 4449 (1982).

⁸R. L. Greene and K. K. Bajaj, *Solid State Commun.* **45**, 852 (1983).

⁹S. Chaudhuri, *Phys. Rev. B* **28**, 4480 (1983).

¹⁰S. Chaudhuri and K. K. Bajaj, *Solid State Commun.* **52**, 967 (1984).

¹¹R. L. Greene and K. K. Bajaj, *Phys. Rev. B* **31**, 913 (1985).

¹²R. L. Greene and K. K. Bajaj, *Phys. Rev. B* **31**, 4006 (1985).

¹³J. A. Brum, C. Priester, and G. Allan, *Phys. Rev. B* **32**, 2378 (1985).

¹⁴N. C. Jarosik, B. D. McCombe, B. V. Shanabrook, J. Comas, J. Ralston, and G. Wicks, *Phys. Rev. Lett.* **54**, 1283 (1985).

¹⁵W. T. Masselink, Y. C. Chang, and H. Morkoç, *Phys. Rev. B* **28**, 7373 (1983).

¹⁶W. T. Masselink, Y. C. Chang, and H. Morkoç, *J. Vac. Sci. Technol. B* **2**, 376 (1984).

¹⁷J. M. Luttinger, *Phys. Rev.* **102**, 1030 (1956).

¹⁸The notation used here is slightly different than that of Ref. 15. Specifically, the $\Gamma_8^{3/2}$ and $\Gamma_8^{1/2}$ states are interchanged and the $\Gamma_8^{-3/2}$ and $\Gamma_8^{-1/2}$ states are interchanged. The D_{2d} Γ_6 and Γ_7 representations are also defined oppositely. The coordinate system used here is related to that of Ref. 15 by the transformation $x \rightarrow y$ and $y \rightarrow -x$.

¹⁹H. C. Casey and M. B. Panish, *Heterostructure Lasers* (Academic, New York, 1978), Vol. 2, p. 16.

²⁰G. F. Koster, J. O. Dimmock, R. G. Wheeler, and H. Statz, *Properties of the Thirty-Two Point Groups* (MIT Press, Cambridge, 1963).

²¹As compiled by J. C. M. Henning, J. J. P. Noijen, and A. G. M. den Nijs, *Phys. Rev. B* **27**, 7451 (1983).

²²R. L. Greene and K. K. Bajaj, *Solid State Commun.* **45**, 831 (1983).

²³D. Gammon and R. Merlin (private communication).

²⁴R. C. Miller, A. C. Gossard, W. T. Tsang, and O. Munteanu, *Phys. Rev. B* **25**, 3871 (1982).

²⁵R. C. Miller, A. C. Gossard, W. T. Tsang, and O. Munteanu, *Solid State Commun.* **43**, 519 (1982).

²⁶M. Altarelli and N. O. Lipari, *Phys. Rev. B* **9**, 1733 (1974).

²⁷P. Lawaetz, *Phys. Rev. B* **4**, 3460 (1971).

²⁸C. Aldrich and R. L. Greene, *Phys. Status Solidi B* **93**, 343 (1979).

²⁹K. Suzuki and J. C. Hensel, *Phys. Rev. B* **9**, 4184 (1974), and references therein.

³⁰C. W. Garland and K. C. Park, *J. Appl. Phys.* **33**, 759 L (1962).

³¹M. Chandrasekar and F. M. Pollak, *Phys. Rev. B* **15**, 2127 (1977).